ACS central science

http://pubs.acs.org/journal/acscii

Outlook

Toward Efficient Electrocatalytic Oxygen Evolution: Emerging Opportunities with Metallic Pyrochlore Oxides for Electrocatalysts and Conductive Supports

Myeongjin Kim,* Jinho Park, Minsoo Kang, Jin Young Kim, and Seung Woo Lee*

Cite This: *ACS Cent. Sci.* 2020, 6, 880−891

Read Online

ACCESS | Metrics & More | Article Recommendations

ABSTRACT: The design of active and stable electrocatalysts for oxygen evolution reaction is a key enabling step toward efficient utilization of renewable energy. Along with efforts to develop high-performance electrocatalysts for oxygen evolution reaction, pyrochlore oxides have emerged as highly active and stable materials that function as catalysts as well as conductive supports for hybrid catalysts. The compositional flexibility of pyrochlore oxide provides many opportunities to improve electrocatalytic performance by manipulating material structures and properties. In this Outlook, we first discuss the recent advances in developing metallic pyrochlore oxides as oxygen evolution catalysts, along with elucidation of their reaction mechanisms, and then introduce an emerging area of using pyrochlore oxides as conductive supports to design hybrid catalysts to further improve the OER activity. Finally, the remaining challenges and emerging opportunities for pyrochlore oxides as electrocatalysts and conductive supports are discussed.

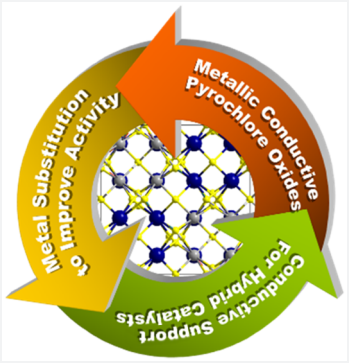

INTRODUCTION

Toward a clean and sustainable energy infrastructure, large-scale energy conversion and storage technologies that can enable efficient utilization of renewable energy are essential. To this end, hydrogen production through the electrochemical water splitting process has been considered as a key technology for storing renewable energy in the form of chemical fuels.[1,2] In water electrolyzers, hydrogen is generated through the reduction of two protons at the cathode; however, the overall efficiency is determined by the slow kinetics of the oxygen evolution reaction (OER), which is the four-proton, four-electron oxidation of water, at the anode.[3,4] Thus, the development of more active and durable OER catalysts has a direct impact on device efficiency and cost-effectiveness.[2,3,5−12]

Substantial efforts have been devoted to the study of various metal oxides, including rutile, spinel, perovskite, rock salt, and bixbyite transition metal oxides, in order to find more efficient catalysts for the OER and to elucidate the reaction mechanisms.[2,4−9,11−14] However, under harsh acidic conditions, candidates for these catalysts are limited to noble metal oxides, such as IrO_2, RuO_2, their solid solutions, Ir- or Ru-based perovskites, and Ruddlesden−Popper phases.[15−21] RuO_2 represents the most active electrocatalyst for the acidic OER, but the dissolution rate of Ru is somewhat faster than Ir in acidic environments.[16,22] IrO_2 exhibits a higher stability than RuO_2 and good activity in acidic medium, but its cost is more than 10 times that of RuO_2.[23] Therefore, various strategies have been attempted to enhance the activity and stability of the Ru- and Ir-based catalysts under acidic conditions by engineering their size, shape, or elemental composition or employing stable substrate materials.[4,8,14,16,24−26] However, the high cost of Ru and Ir still limits the large-scale application of proton exchange membrane water electrolyzers.[25]

The crystal family of pyrochlore is a complex oxide with a general formula of $A_2B_2O_{7-\delta}$ of which A is usually an alkaline-earth or rare-earth element and B is a transition metal.[15] Recently, iridium and ruthenium pyrochlore oxides, $A_2B_2O_{7-\delta}$ (B = Ir or Ru), have risen as promising alternatives to binary RuO_2 and IrO_2 oxides because of the low content of noble metal, high activity, and stability under both alkaline and acidic conditions.[15,22,23,27−38] Based on its crystal structure, the formula of pyrochlore oxides also can be described as $(A_2B_2O_6O')$ or $[A_2O'][B_2O_6]$ with two types of oxygen, consisting of a network of corner-sharing BO_6 octahedra with A and O′ atoms occupying interstitial sites (A_2O') (Figure 1).[28] Thus, the O anion connects two building blocks to form a network between the A- and B-site cations, while the O′ anion links only to the A-site cations in the form of A−O′−A.[28] It is known that oxygen vacancies are generally formed preferentially at the interstitial O′ sites rather than at the O sites.[38] Thanks to

Received: April 20, 2020
Published: June 5, 2020

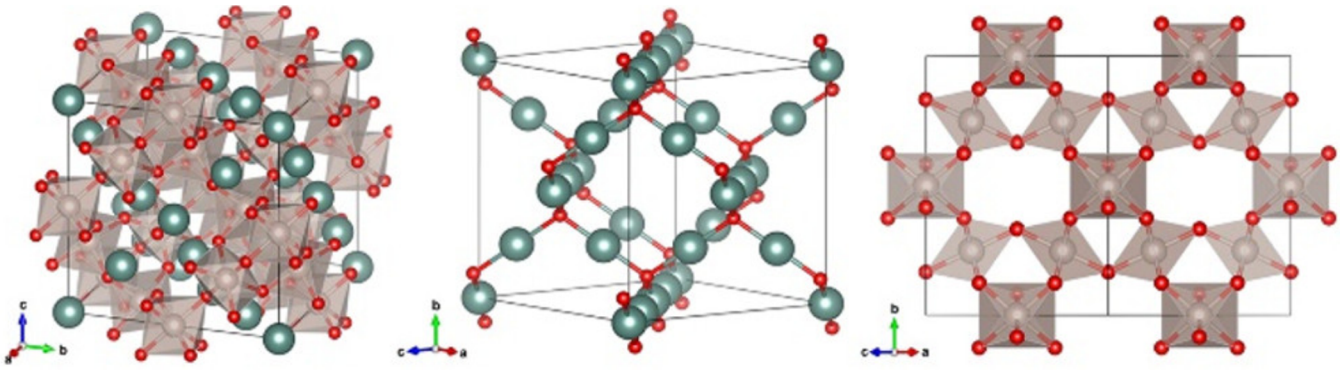

Figure 1. Unit cell structure of $A_2B_2O_7$ (left) showing the A_2O' chains (middle) and corner shared octahedral BO_6 structures (right). Color code: A (teal), B (gray), and O (red).[28] Images reproduced with permission from ref 28. Copyright 2017 American Chemical Society.

the compositional flexibility of the A and B sites to manipulate their wide spectrum of properties, including electrical, magnetic, dielectric, optical, and electrocatalytic properties, pyrochlores have been used in a variety of applications, such as ionic/electrical conductors, anode materials for solid electrolyte fuel cells, radioactive waste immobilization, high-temperature thermal barrier coatings, photocatalysts, electrocatalysts for oxygen reduction reaction (ORR), and OER.[39−41] In particular, pyrochlore oxides with metallic conduction behavior are attractive candidates for OER catalysts due to their high conductivity, fast charge transfer through the oxygen vacancies, and structural stability. In addition, the ability to substitute different ions into the A- and B-site elements while maintaining the same crystal structure provides another powerful strategy to tune the concentration of oxygen vacancies and electronic structures, and thus the OER activity and stability.

In particular, pyrochlore oxides with metallic conduction behavior are attractive candidates for OER catalysts due to their high conductivity, fast charge transfer through the oxygen vacancies, and structural stability.

In this Outlook, we first briefly summarize the recent advances in designing metallic pyrochlore oxides as OER catalysts through composition control of A- and B-site cations, along with elucidation of their OER mechanisms and structure−mechanism−performance relationship. Then, we introduce a new approach using metallic pyrochlore oxides as conductive supports to design hybrid catalysts using the *in situ* exsolution method, highlighting the synergetic effects between catalyst and support to enhance the OER activity. Finally, we discuss the remaining challenges and emerging opportunities of pyrochlore oxides as electrocatalysts and conductive supports.

METALLIC PYROCHLORE OXIDES AS OXYGEN EVOLUTION REACTION CATALYSTS

Bismuth (Bi) and lead (Pb) pyrochlores have been identified as metallic conductors.[42,43] It was first suggested that the metallic behavior of $Pb_2Ru_2O_{7-\delta}$ is due to the significant mixing between Ru 4d, Pb 6s, and Pb 6p bands.[43−45] Later, Hsu and co-workers showed that the Pb 6s band was unlikely to contribute to the metallic behavior, but the metallic conductivity of $Bi_2Ru_2O_7$ and $Pb_2Ru_2O_{6.5}$ was due to the mixing of unoccupied Pb (or Bi) 6p and Ru 4d bands via the ligand oxygen 2p states. In general, the metallic vs semiconductor behavior of ruthenium pyrochlores ($A_2Ru_2O_{7-\delta}$) can be determined by the Mott−Hubbard mechanism of electron localization.[46] Since the width of the t_{2g}-block bands of $A_2Ru_2O_{7-\delta}$ increases as the Ru−O−Ru bond angle increases, the structure exhibits metallic behavior when the Ru−O−Ru bond angle is larger than 133°.[46] In addition, there is a strong linear relationship between the ionic radius of the A-cation and the Ru−O−Ru bond angle, explaining the metallic behavior of ruthenium pyrochlores with large size cations such as Bi, Pb, and Tl.[46] Such metallic conductivity of pyrochlore oxides allows the preparation of self-supported electrodes without the use of conductive carbon support, simplifying membrane electrode assembly in water electrolyzers.[38] Motivated by this highly conductive behavior, metallic pyrochlores, $A_2B_2O_{7-\delta}$ (A = Bi, Pb, Tl, B = Ru, Ir) have been actively investigated as OER catalysts under both alkaline and acidic conditions.[22,27,38,47−52]

Ramani and co-workers synthesized conductive pyrochlore oxides ($A_2B_2O_{7-\delta}$, A = Pb or Bi and B = Ru, Ir or Os) using solid-state methods and compared their OER activities in 0.1 M KOH.[38] They correlated the OER activity trend (ruthenate pyrochlores > iridate pyrochlores > osmate pyrochlores) with the bonding strength between the B-site cation and the oxygen species based on the conventional OER mechanism established by density functional theory (DFT) calculations on metal oxides.[3,9,13] Based on a single descriptor, the oxygen adsorption energy on the catalyst surface, the conventional OER mechanism follows the Sabatier principle: the best catalyst binds oxygen on its surface neither too weakly nor too strongly.[3,9,13] Among binary oxides, RuO_2 and Co_3O_4 exhibit the lowest theoretical overpotentials because of their optimal binding energy of oxygen (Figure 2a).[3,13] Based on this mechanism, they employed the calculated d-band center and adsorbate (s or p)−metal d-coupling matrix element squared, V_{ad}^2,[53] to explain the high activity of ruthenate pyrochlores through their optimum interaction with oxygen intermediates.[38]

Current understanding of transition metal oxide-based OER catalysts suggests that increasing the covalency of the transition metal (TM)−O bond can lower the energy associated with O−O bond formation,[6,54,55] which is often considered as the rate-determining step for the conventional OER mechanism.[9,13] Therefore, the effects of the covalency of the TM−O bonds on the OER activities have been studied for Ru and Ir pyrochlore oxides.[33,35] Cho and co-workers reported that the covalency of

https://dx.doi.org/10.1021/acscentsci.0c00479
ACS Cent. Sci. 2020, 6, 880−891

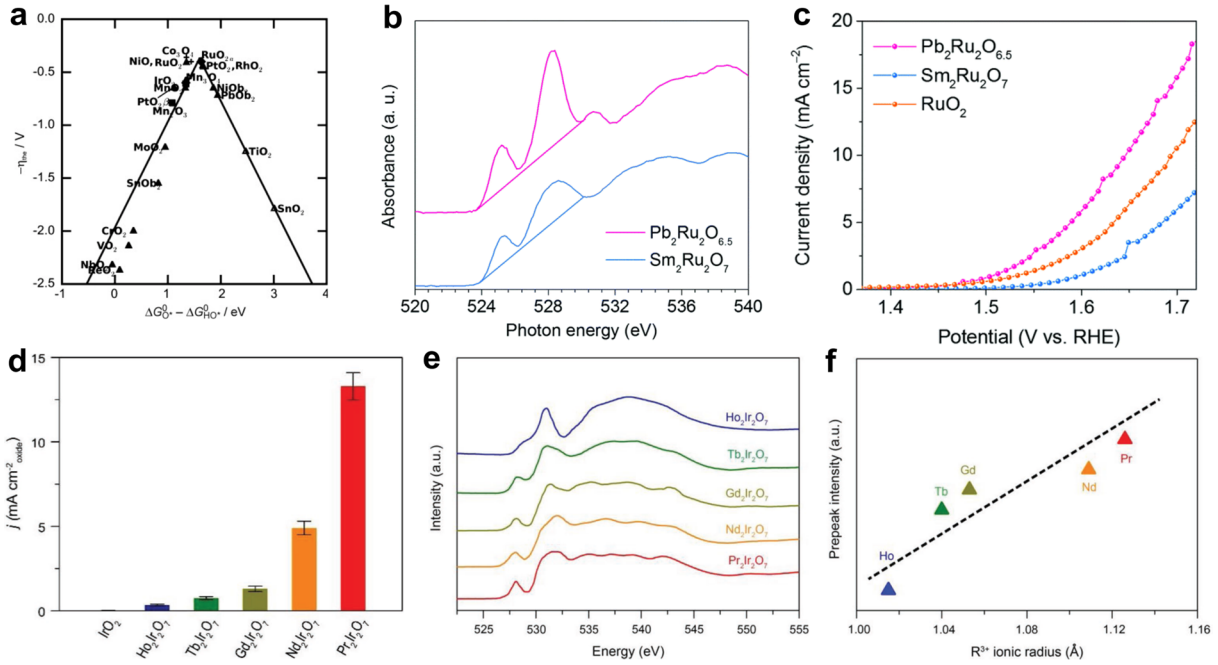

Figure 2. (a) Activity trends toward oxygen evolution for binary oxides.[13] (b) *Ex situ* normalized O K-edge XANES total electron yield mode spectra of the highly crystalline pyrochlore oxides ($A_2Ru_2O_{7-x}$, A = Pb and Sm).[35] (c) Linear scan voltammogram curves showing the OER activities of pyrochlore oxides and RuO_2 in 0.1 M KOH.[35] (d) Specific OER activity of pyrochlore oxides at η = 300 mV in 0.1 M $HClO_4$.[33] (e, f) O K-edge XAS and the normalized intensity of the prepeak around 528 eV.[33] Images reproduced with permission from refs 13, 35, and 33. Copyright 2011 WILEY-VCH, 2017 The Royal Society of Chemistry, 2018 WILEY-VCH.

Ru−O bonds of ruthenate pyrochlores affected the ORR and OER activities by comparing the X-ray absorption near edge structure (XANES) spectra of the insulating $Sm_2Ru_2O_7$ and metallic $Pb_2Ru_2O_{6.5}$.[35] The degree of covalency of Ru−O bonds on the surface of the pyrochlore oxides was quantified based on the O K-edge XANES spectra at total electron yield mode (Figure 2b) with the equation of absorbance/($hole_{eg}$ + 1/4$hole_{t2g}$).[35] The higher covalency value of metallic $Pb_2Ru_2O_{6.5}$ (0.65) than that of insulating $Sm_2Ru_2O_7$ (0.39) strengthened was correlated with the higher OER activity of $Pb_2Ru_2O_{6.5}$ compared to $Sm_2Ru_2O_7$ in 0.1 M KOH (Figure 2c). In addition, Shang et al. studied the electronic structures of a series of pyrochlore iridates ($R_2Ir_2O_7$) with different sizes of rare earth cations (R = Ho < Tb < Gd < Nd < Pr) in correlation with their OER activities under acidic conditions.[33] The OER activity of iridate pyrochlores in 0.1 M $HClO_4$ gradually increased with the R ionic radius (Figure 2d).[33] In particular, $Pr_2Ir_2O_7$ showed considerably enhanced activity and stability compared to the benchmark IrO_2.[33] Such enhanced activity of $Pr_2Ir_2O_7$ was attributed to the improved electrical conductivity and the enhancement of Ir−O bond covalency. They showed that increasing R ionic radius weakens the effective electron correlations in these iridate pyrochlore oxides via the chemical pressure effect, inducing an insulator−semimetal−metal transition.[33] The O K-edge XANES spectra (Figure 2e) were used to evaluate the strength of Ir 5d−O 2p orbital hybridization in these oxides.[33] The prepeak intensity at ∼528 eV, which is associated with the transition from the O 1s core level to the unoccupied O 2p states hybridized with Ir 5d t_{2g} orbitals, was compared as an indicator of the metal−oxygen orbital hybridization (Figure 2f).[33] The normalized intensity of the prepeak clearly increased with increasing the ionic radius of R, indicating the enhanced the Ir 5d−O 2p hybridization through the reduced electron correlations (Figure 2f). These results suggest that increasing the Ir−O covalency by adjusting the ionic radius of the A-site cation can be an effective strategy to enhance the OER activity of iridate pyrochlores.

Taking into account that numerous pyrochlore oxides can be generated from various combinations of A-site and B-site components, the computation-based screening process is critical to identify the ideal structure and property of pyrochlore having superior catalytic activity and stability. Schmidt and co-workers first employed a computational method to investigate a series of lanthanide pyrochlore oxides ($A_2B_2O_7$, A = La, Ce, Pr, Nd, Sm, Gd, or Yb and B = Ir or Ru) as OER catalyst candidates.[31] Specifically, the phase diagrams, Pourbaix diagrams (potential vs pH), band energy diagrams, and projected density of states (PDOS) were calculated for these pyrochlore oxides to investigate their phase stability, electrochemical stability, conductivity, and Ir 5d or Ru 4d−O 2p hybridization, respectively (Figure 3).[31] Using the calculated phase diagram (Figure 3a) and total energy (eV/atoms) for these pyrochlores, it was possible to predict whether materials could be synthesized. In addition, the calculated Pourbaix diagrams were used to determine whether materials will dissociate at the pH and electrochemical potential values under OER conditions. For example, the Pourbaix diagram of $Gd_2Ir_2O_7$ pyrochlore shows that this material does not dissolve when contacted with water under OER conditions (Figure 3b).[31] Moreover, the band structure diagram of $Gd_2Ir_2O_7$ shows that the material can be considered conductive because some bands intersect at the Fermi level (Figure 3c).[31] The PDOS shows that, for most pyrochlore candidates, the valence band is formed by the Ir or Ru d-orbitals hybridized with the O 2p orbitals and the Ir or Ru d-orbitals also contribute to the conduction band, which is sometimes hybridized with the A-site element f-orbitals (Figure 3d).[31] Based on these systematic screening processes, only a few materials ($A_2B_2O_7$, A = Nd, Gd, or Yb and B = Ir or Ru) were

https://dx.doi.org/10.1021/acscentsci.0c00479
ACS Cent. Sci. 2020, 6, 880−891

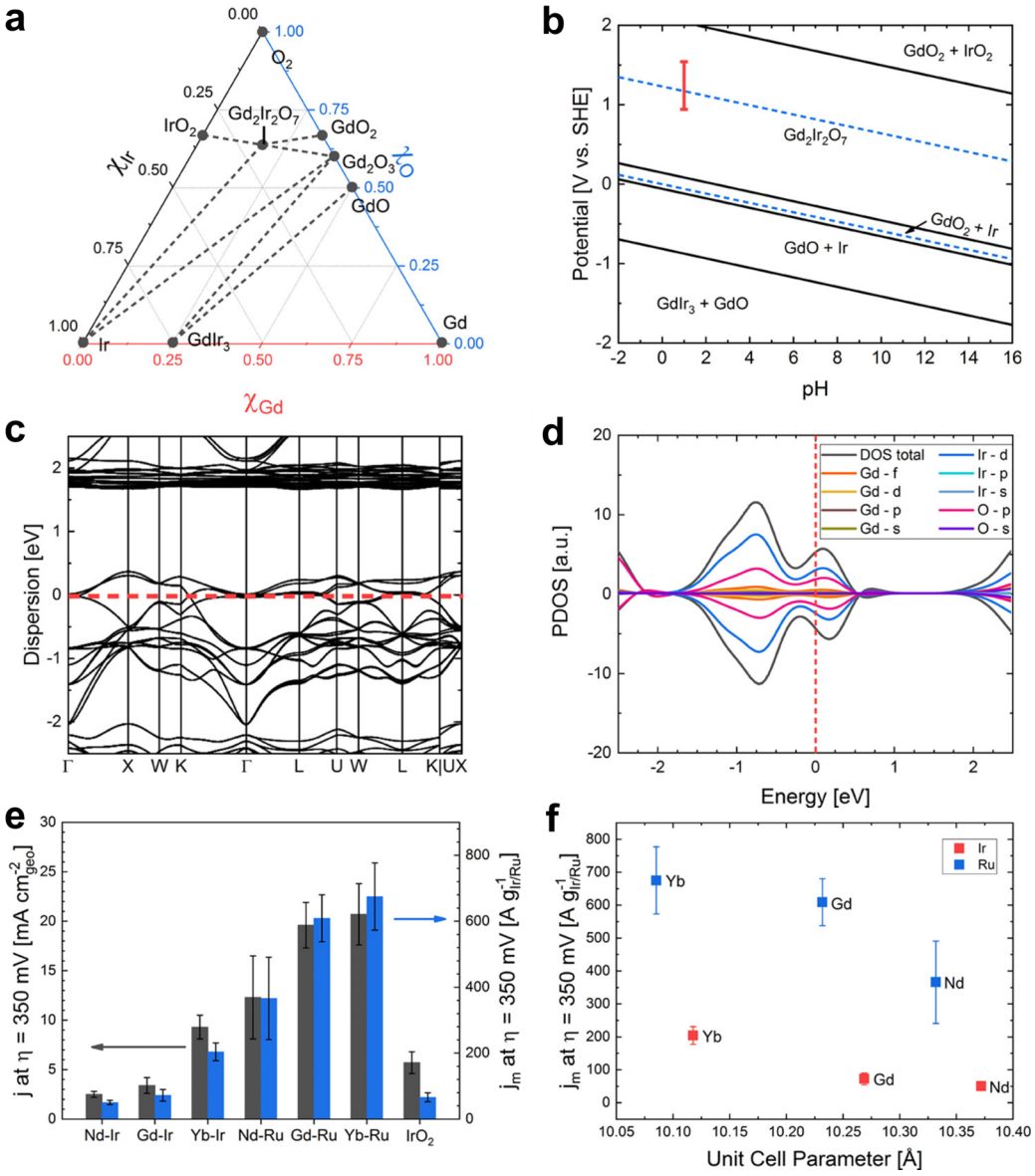

Figure 3. (a) Phase diagram, (b) Pourbaix diagram, (c) band structure diagram, and (d) PDOS diagram for $Gd_2Ir_2O_7$.[31] (e) Measured OER activities for the Ru and Ir pyrochlore series in 0.1 M $HClO_4$ and (f) average specific activity of the pyrochlore oxides as a function of the unit cell parameter.[31] Images reproduced with permission from ref 31. Copyright 2019 American Chemical Society.

identified for the synthesis and testing as OER catalysts.[31] $Yb_2Ir_2O_7$ and the ruthenate pyrochlores ($Nd_2Ru_2O_7$, $Gd_2Ru_2O_7$, and $Yb_2Ru_2O_7$) exhibited higher OER activity and stability in 0.1 M $HClO_4$ compared to the IrO_2 catalyst (Figure 3e).[31] The OER activity of iridate or ruthenate pyrochlore series generally increased with decreasing size of the A-site cation (Figure 3f).[31] It is interesting to note that this trend is the opposite of other pyrochlore iridate systems ($R_2Ir_2O_7$, R = Ho, Tb, Gd, Nd, and Pr, Figure 2d).[33] Despite the opposite trend of these two studies,[31,33] controlling the A-site ion in Ir or Ru pyrochlore oxides suggests an effective strategy in creating stable, conductive, highly active, and stable OER catalysts.

Taking into account that numerous pyrochlore oxides can be generated from various combinations of A-site and B-site components, the computation-based screening process is critical to identify the ideal structure and property of pyrochlore having superior catalytic activity and stability.

METAL SUBSTITUTION FOR PYROCHLORE OXIDES

Metal cation substitution is the most popular strategy to tune the electronic structure of metal oxides by controlling the oxidation state of the metal and the concentration of oxygen vacancy (OV). This strategy has also been actively adopted to enhance the OER activity of pyrochlore oxides, with a particular focus on pyrochlore-type yttrium ruthenate ($Y_2Ru_2O_{7-\delta}$). Yang and co-workers first showed that phase-pure $Y_2Ru_2O_{7-\delta}$ exhibited significantly enhanced OER activity and stability over conven-

https://dx.doi.org/10.1021/acscentsci.0c00479
ACS Cent. Sci. 2020, 6, 880−891

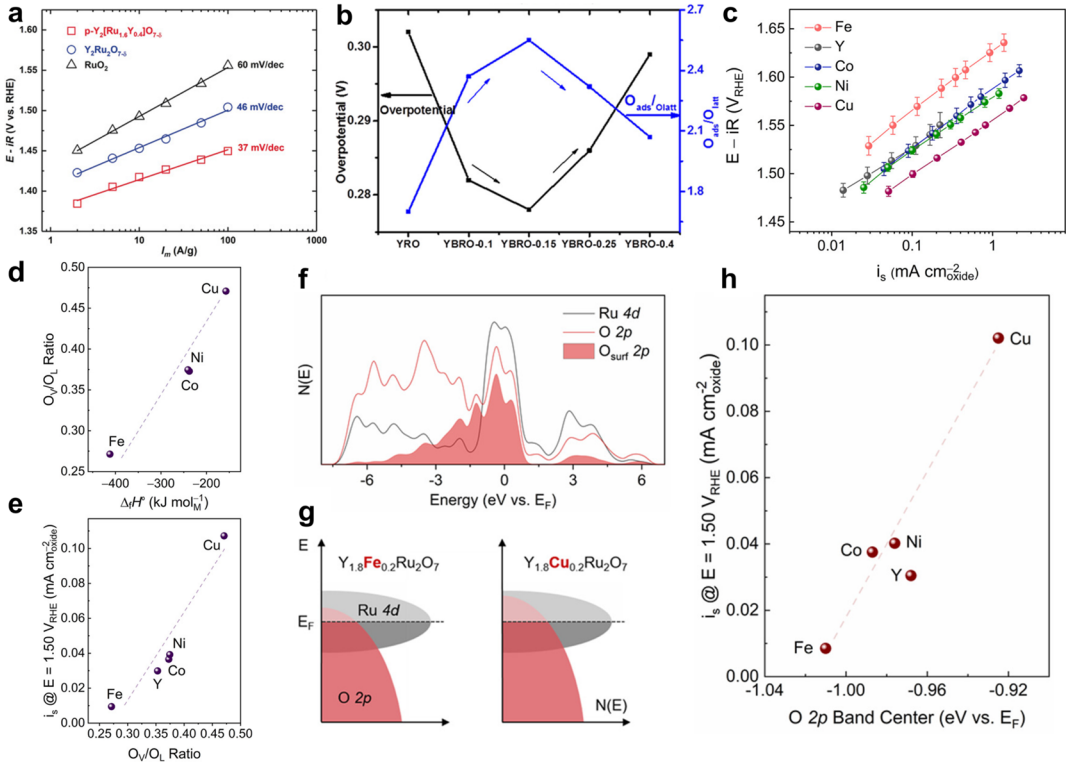

Figure 4. (a) OER activity comparison of porous $Y_2[Ru_{1.6}Y_{0.4}]O_{7-\delta}$, $Y_2Ru_2O_{7-\delta}$, and RuO_2 electrocatalysts in 0.1 M $HClO_4$ by Tafel plots.[30] (b) The relationships between OER overpotential (at 10 mA cm^{-2}) in 0.5 M H_2SO_4 and OV concentration for $Y_{2-x}Ba_xRuO_{7-\delta}$ (x = 0, 0.1, 0.15, 0.25, 0.4).[32] (c) Tafel plots of $Y_{1.8}M_{0.2}Ru_2O_{7-\delta}$ measured in 1 N H_2SO_4.[34] (d) Scaling between OV content expressed as O_V/O_L ratio and enthalpies of MO_x formation, $\Delta_f H°$.[34] (e) Relation between the OER activity of $Y_{1.8}M_{0.2}Ru_2O_{7-\delta}$ and O_V/O_L ratio.[34] (f) PDOS on Ru 4d and O 2p states of $Y_{1.8}Cu_{0.2}Ru_2O_7$. PDOS on O 2p states of surface terminated oxygen atoms (O_{surf}) are shaded.[34] (g) Schematic rigid band diagram for $Y_{1.8}Fe_{0.2}Ru_2O_7$ and $Y_{1.8}Cu_{0.2}Ru_2O_7$ visualizing an upshift of the O 2p band center.[34] (h) Scaling between specific OER activity and O 2p band center position for $Y_{1.8}M_{0.2}Ru_2O_{7-\delta}$.[34] Images reproduced with permission from refs 30, 32, and 34. Copyright 2018 Wiley-VCH, 2020 American Chemical Society.

tional RuO_2 electrocatalysts in 0.1 M $HClO_4$.[28] Later, the same group introduced porous $Y_2[Ru_{1.6}Y_{0.4}]O_{7-\delta}$ through the partial substitution of Ru^{4+} with Y^{3+} cations, demonstrating the improved OER activity compared to $Y_2Ru_2O_{7-\delta}$ (Figure 4a).[30] The enhanced activity of $Y_2[Ru_{1.6}Y_{0.4}]O_{7-\delta}$ was attributed to both the high surface area of the porous material and the introduced oxygen lattice defects that are formed by the mixed oxidation state of $Ru^{4+/5+}$ through partial substitution by Y^{3+} on the B-site.[30] Specifically, they suggested that the oxygen-deficient pyrochlore structure can lower the band energy and strengthen the covalent bond between the Ru 4d band and the O 2p band, which is beneficial for OER performance.[30]

Due to the n-type semiconducting property, phase-pure $Y_2Ru_2O_{7-\delta}$ (YRO) shows low electrical conductivity. Brambilla and co-workers have shown that A-site doping of YRO with Zn^{2+} ($Y_{1.85}Zn_{0.15}Ru_2O_{7-\delta}$) can increase the conductivity by 2 orders of magnitude compared to undoped YRO at room temperature.[56] In addition, previous studies have shown that doping the A-site of pyrochlores with 2+ cation can lead to a hole doping effect with an increased concentration of disordered oxygen vacancies (OVs).[56−58] Motivated by these doping effects, Wang and co-workers have reported a series of A-site-doped YRO pyrochlores ($Y_{2-x}A_xRuO_{7-\delta}$, A= Zn,[23] Ca,[59] Ba,[32] and Mg[60]) as highly active and stable OER catalysts. The substitution of 2+ cation at the A-site of YRO enables the formation of OVs and mixed valences of $Ru^{5+/4+}$, which significantly alters the electronic structure and conductivity. Figure 4b shows the strong correlation between the OV concentration of $Y_{2-x}Ba_xRuO_{7-\delta}$ (x = 0, 0.1, 015, 0.25, and 0.4) and their OER activities in 0.5 M H_2SO_4.[32] They explain that a higher OV concentration in the catalysts can provide more adsorption sites for the OER intermediates.[32] Moreover, the hole-doping effect caused by the A-site doping of YRO catalysts can enhance conductivity, generate multivalence of $Ru^{5+/4+}$, and alter the electronic band structure, which can all benefit the OER activity.[32]

Since the metal substitution can cause several structural changes, including OV concentration, conductivity, and electronic band structure, it is critical to evaluate the contribution of each variable to the OER activity and stability. To answer this important question, Müller and co-workers have studied model pyrochlores of $Y_{1.8}M_{0.2}Ru_2O_{7-\delta}$ (M = Cu, Co, Ni, Fe, and Y) as OER catalysts in acid.[34] Using a moderate level of A-site substitution, the oxidation state of Ru was maintained unchanged within the series, which is intended to study the individual effect of the M substituent on the OER activity.[34] Similar Tafel slopes (52−63 mV/dec) of all prepared pyrochlores indicate the same rate-limiting step (Figure 4c), but the specific OER activity of $Y_{1.8}Cu_{0.2}Ru_2O_{7-\delta}$ at 1.50 V vs reversible hydrogen electrode (RHE) in 1 N H_2SO_4 is more than 1 order of magnitude higher than $Y_{1.8}Fe_{0.2}Ru_2O_{7-\delta}$.[34] The concentration of surface OVs in the pyrochlore was calculated based on the ratio of O_V (oxygen vacancy)/O_L (lattice oxygen) through O 1s core level X-ray photoelectron spectroscopy (XPS) spectra. The calculated concentration of OV sites showed good correlations with the enthalpy of formation of the binary oxides MO_x (Figure 4d) and the OER activity (Figure 4e).[34] These trends were explained by comparing the electronic band

https://dx.doi.org/10.1021/acscentsci.0c00479
ACS Cent. Sci. 2020, 6, 880−891

structures of pyrochlores. The calculated density of states (DOS) of $Y_{1.8}M_{0.2}Ru_2O_7$ showed a substantial contribution of oxygen states to the bands near the Fermi level (E_F) (Figure 4f), indicating the high covalency of the Ru−O bonds.[34] Transitioning the substitution from Fe to Y, Ni, Co, and to Cu at the A-site shifted the E_F closer to the O 2p band center and also decreased the energy gap between the Ru 4d and O 2p band centers,[34] defined as charge transfer energy from the previous study on perovskite catalysts.[61] As the E_F moves down closer to the O 2p states, the states below the E_F show a greater oxygen character, indicating a higher covalency of the Ru−O bond in $Y_{1.8}Cu_{0.2}Ru_2O_7$ compared to $Y_{1.8}Fe_{0.2}Ru_2O_7$ (Figure 4g).[34] A strong correlation between OV concentration and O 2p band center relative to the E_F was reported for perovskite catalysts.[62] Therefore, the upshift of the O 2p band center relative to the E_F can explain the higher concentration of OV in $Y_{1.8}Cu_{0.2}Ru_2O_7$ (Figure 4g). In addition, the OER activity of $Y_{1.8}M_{0.2}Ru_2O_7$ pyrochlores strongly correlated with the O 2p band center relative to the E_F computed for surface O atoms (Figure 4h).[34] Therefore, the enhanced OER activity of $Y_{1.8}Cu_{0.2}Ru_2O_7$ was attributed to the decreased energy gap between the O 2p states and the E_F as well as the reduced charge transfer energy.

UNDERSTANDING OF OXYGEN EVOLUTION REACTION MECHANISMS ON PYROCHLORE OXIDES

The conventional OER mechanism of metal oxides is derived from that of metal catalysts, where the dominant parameter governing the reaction overpotential is the binding strength of oxygenated adsorbates (Figure 5, adsorbate evolution mecha-

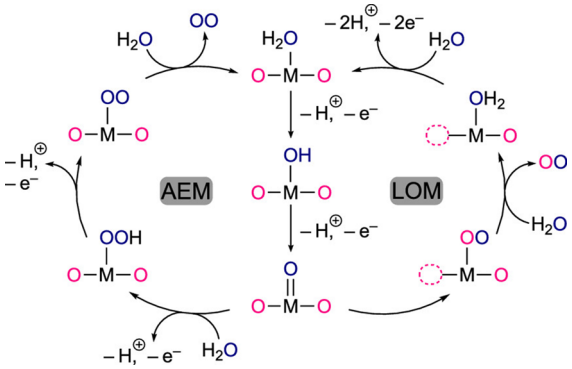

Figure 5. Schematic illustration showing OER mechanisms under acidic conditions: adsorbate evolution mechanism (AEM) and lattice-oxygen-mediated mechanism (LOM).[34] An image reproduced with permission from ref 34. Copyright 2020 American Chemical Society.

nism (AEM)).[9,12,13,34] The scaling relationship between adsorption energies of the oxygenated adsorbates defines a theoretical minimum overpotential for the OER.[13] Recent studies on metal oxide catalysts have suggested the possibility of a different reaction mechanism based on the involvement of lattice oxygens in the OER, the so-called lattice oxygen(-mediated) mechanism (LOM, Figure 5).[3,5,34,63−65] This LOM mechanism involves the oxidation of the lattice oxygen (more precisely, the lattice O^{2-} anions), thus avoiding the scaling limitations of the conventional AEM.[3,34] Therefore, understanding the LOM mechanism on pyrochlore oxides is important to improve the OER kinetics. Schmidt and co-workers first investigated the contribution of the LOM mechanism on highly crystalline pyrochlores ($Yb_2Ru_2O_7$ and $Gd_2Ru_2O_7$) by measuring the isotopic distribution of the evolved oxygen in ^{18}O-labeled water using differential electrochemical mass spectrometry (DEMS).[31] Assuming that the surface of the pyrochlore is composed of solely ^{16}O, the LOM mechanism can produce the $^{16}O^{18}O$ or $^{16}O_2$ through the participation of the pyrochlore lattice oxygen.[31] Two types of molecular oxygen ($^{18}O_2$ with m/z of 36 and $^{16}O^{18}O$ with m/z of 34) were detected, but the ratio of $^{16}O^{18}O$ (m/z = 34) was only 0.04, indicating the negligible contribution of the LOM mechanism.[31] A recent study also showed no involvement of the lattice oxygen on crystalline RuO_2 films during OER, suggesting that the LOM mechanism can only be involved with amorphous RuO_2 or nanocrystalline phases with under-coordinated edge sites.[66]

Although highly crystalline pyrochlores showed negligible involvement of the lattice oxygen in the OER, the LOM mechanism may play a role on the doped pyrochlores containing large amounts of oxygen vacancies. Recent studies have also suggested an important role of OVs in the LOM mechanism of perovskite catalysts.[3,67,68] In agreement with this suggestion, Müller and co-workers hypothesized that the increased oxygen lability and surface density of OV in pyrochlores favored the LOM mechanism, which may increase the OER activity.[34] Using model pyrochlores of $Y_{1.8}M_{0.2}Ru_2O_{7-\delta}$ (M = Cu, Co, Ni, and Fe), they suggested that the enthalpy of formation ($\Delta_fH°$) of the binary oxides MO_x (Fe_2O_3, CoO, NiO, and CuO) can be an important parameter to understand the relationship between the surface oxygen lability and the OER activity. The calculated $\Delta_fH°$ of the binary oxides MO_x showed a strong correlation with the density of OV site and the OER activity of $Y_{1.8}M_{0.2}Ru_2O_7$ pyrochlores (Figure 4d and e). The less negative $\Delta_fH°$ of MO_x indicates the weaker M−O bonds (i.e., less stable oxide) that can promote the removal of lattice oxygen atoms. Therefore, $Y_{1.8}Cu_{0.2}Ru_2O_7$ with the smallest negative value of $\Delta_fH°$ of MO_x showed the highest concentration on OV and ultimately the highest OER activity.[34] These results indicate that $\Delta_fH°$ of a bulk binary oxide can be a useful parameter to understand the LOM mechanism in correlation with surface oxygen lability and density of OV in pyrochlores.

> Although highly crystalline pyrochlores showed negligible involvement of the lattice oxygen in the OER, the LOM mechanism may play a role on the doped pyrochlores containing large amounts of oxygen vacancies.

PYROCHLORE OXIDE SUPPORTS FOR HYBRID CATALYSTS

Carbon blacks, such as Ketjenblack (AkzoNobel) and Vulcan (Cabot), have been dominantly used as supports for electrocatalysts due to their high electric conductivity (~20 S/cm) and high surface area (200−800 m^2/g).[69,70] However, the carbon black support is highly corroded under OER conditions, resulting in the detachment of active catalytic materials from the support.[69−71] Although graphitized carbon is more durable than porous carbon black, it still suffers from irreversible oxidation at high potential and acidity.[69] Metal oxides have been

https://dx.doi.org/10.1021/acscentsci.0c00479
ACS Cent. Sci. 2020, 6, 880−891

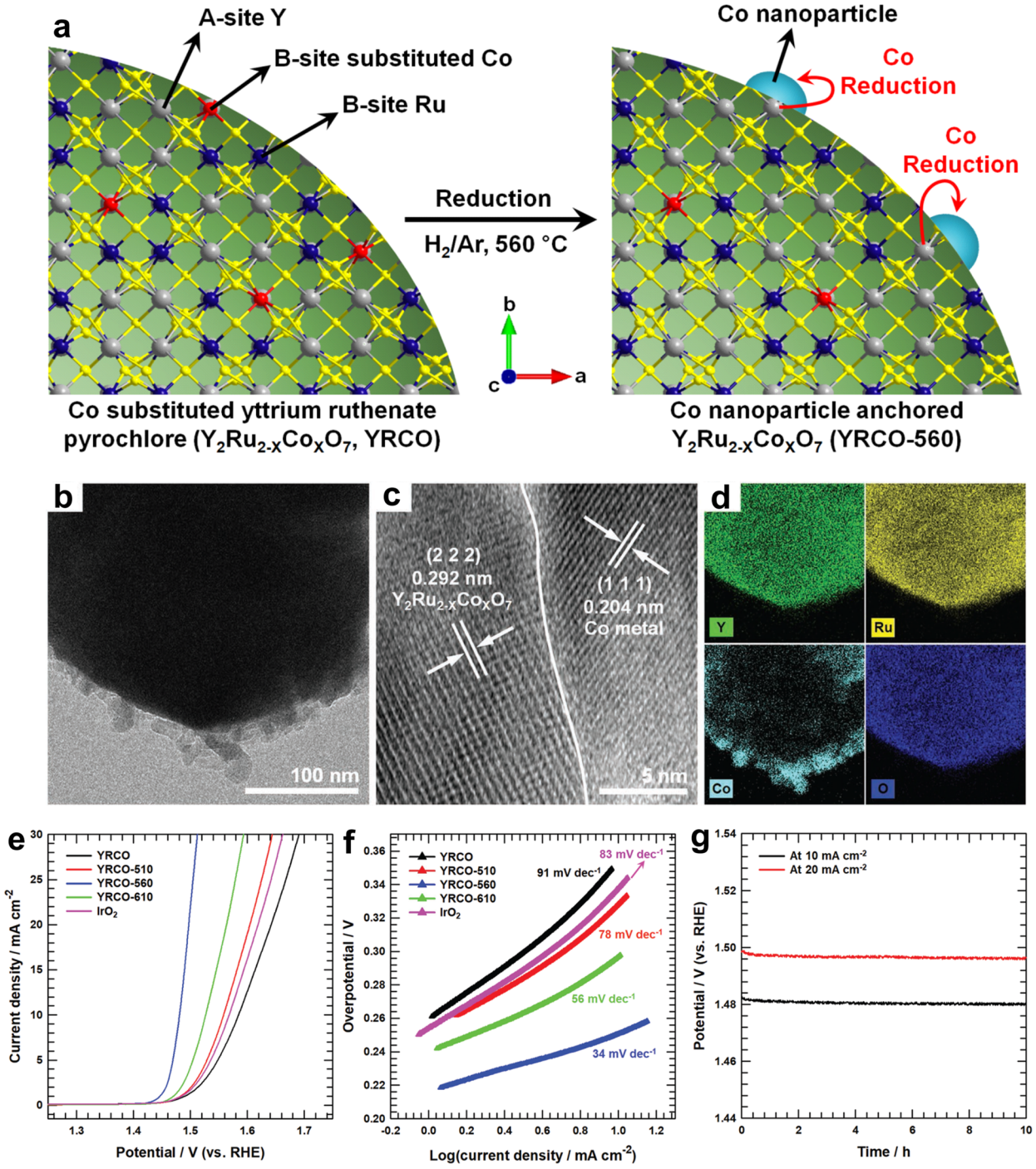

Figure 6. (a) Schematic illustration synthesis of YRCO-560 via the *in situ* exsolution of Co nanoparticles from $Y_2Ru_{2-x}Co_xO_7$ at 560 °C under a mixture of H_2/Ar gases.[78] (b, c) Transmission electron microscopy (TEM) images of YRCO-560.[78] (d) Scanning TEM energy dispersive X-ray mapping images for Y, Ru, Co, and O elements distributed at the YRCO-560.[78] (e) OER polarization curves and (f) Tafel plots for YRCO-560 and IrO_2 in 0.1 M KOH.[78] (g) Chronopotentiometric tests for YRCO-560 at 10 and 20 mA/cm^2 for 10 h.[78] Images reproduced with permission from ref 78. Copyright 2019 WILEY-VCH.

considered as alternative supports for OER, with enhanced conductivity through metal doping.[69,72,73] In particular, metallic pyrochlore oxides, such as $Pb_2Ru_2O_{7-\delta}$, exhibit a high conductivity of $(2-5) \times 10^3$ S/cm.[45] For example, the recently reported conductive pyrochlore oxides ($A_2B_2O_{7-\delta}$, A = Pb or Bi and B = Ru, Ir, or Os) showed high conductivity in the range of 50−120 S/cm.[38] Additionally, A-site doping of semiconducting YRO with Zn^{2+} or Ca^{2+} increases the conductivity to 0.1−50 S/cm.[56,74] Such high conductivity of pyrochlore oxides is sufficient to meet the minimum electric conductivity requirement (∼0.1 S/cm)[69] for electrocatalytic support applications. In addition to high electric conductivity, the synthesis of nanoscale pyrochlore oxides is also important for both electrocatalyst and support applications. Conventional solid-state synthesis of pyrochlore oxides is typically performed at high calcination temperatures above 800 °C, resulting in micron-scale products with low surface area.[38] Therefore, significant efforts have been made to synthesize nanoscale pyrochlore oxides using various methods,

https://dx.doi.org/10.1021/acscentsci.0c00479
ACS Cent. Sci. 2020, 6, 880−891

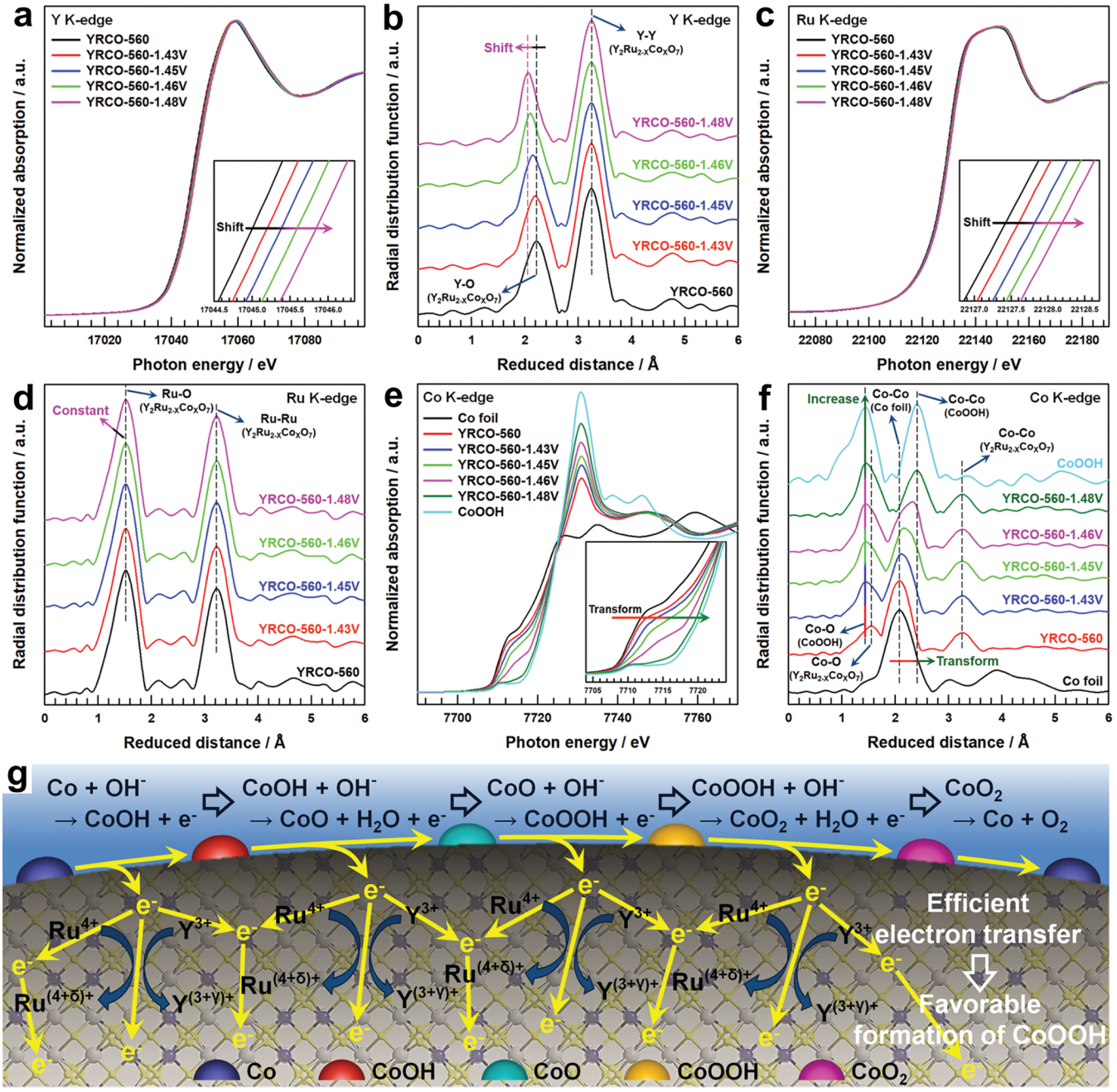

Figure 7. *In situ* (a, b) Y, (c, d) Ru, and (e, f) Co K-edge XANES and EXAFS spectra of YRCO-560 from 1.43 to 1.48 V vs RHE in 0.1 M KOH.[78] (g) Schematic of the efficient electron transfer characteristic of YRCO-560 during OER.[78] Images reproduced with permission from ref 78. Copyright 2019 WILEY-VCH.

including hydrothermal synthesis,[27] sol−gel process,[35] templating approach,[75] Adams fusion method,[15] glycine-nitrate combustion method,[76] perchloric acid-based porogen method,[30] and polymer entrapment flash pyrolysis method.[77] These efforts allow the size of pyrochlore oxides to be reduced to tens of nanometers with significantly improved surface area, making them more qualified catalysts and conductive supports.

While most of the reported works have focused on the use of pyrochlore oxides as active OER catalysts, a recent study first showed that pyrochlore oxide can be a promising substrate for depositing other transition metal catalysts to design high-performance hybrid catalysts.[78] Kim et al. have designed the metallic cobalt (Co) nanoparticles anchored pyrochlore oxide hybrid catalysts through the *in situ* exsolution process of Co substituted yttrium ruthenate pyrochlore oxide ($Y_2Ru_{2-x}Co_xO_7$) (Figure 6a). Through careful control of the reduction temperature, metallic Co nanoparticles were formed on the surface of $Y_2Ru_{2-x}Co_xO_7$ pyrochlore without collapsing the crystal structure of the pyrochlore oxide support (Figure 6b−d).[78] The synthesized Co nanoparticles decorated $Y_2Ru_{2-x}Co_xO_7$ catalyst (YRCO-560) exhibited superior OER activity and stability in 0.1 M KOH (Figure 6e−g).[78]

The *in situ* X-ray absorption spectroscopy (XAS) technique was employed for in-depth understanding of the origin of the superior OER performance of this hybrid catalyst (YRCO-560). While the applied potential increased, the Y K-edge XANES spectra were positively shifted and the Y−O bonds peak in the Y K-edge extended X-ray absorption fine structure (EXAFS)

https://dx.doi.org/10.1021/acscentsci.0c00479
ACS Cent. Sci. 2020, 6, 880−891

spectra were negatively shifted, clearly indicating the oxidation behavior of Y cations in YRCO-560 under OER conditions (Figure 7a and b).[78] The oxidation of Ru cations at the B-site in YRCO-560 was also confirmed by observing the positively shifted Ru K-edge XANES spectra with increasing potential (Figure 7c).[78] Such facile oxidation behavior of the Y and Ru cations may infer efficient charge transfer from the surface to the inner layer of pyrochlore oxide during the OER process.[78] In addition, the reduced distance of Ru−O bonds in the Ru K-edge EXAFS spectra showed negligible changes under OER conditions (Figure 7d).[78] Such rigid B-site RuO_6 octahedral frameworks can contribute to the high stability of YRCO-560 during the OER process.[36] Both the decreased pre-edge peak intensity and the positively shifted absorption edge in the Co K-edge XANES spectra of YRCO-560 (Figure 7e) indicate the transformation of metallic Co nanoparticles to CoOOH during the OER process.[78] The Co K-edge EXAFS spectra of YRCO-560 showed a Co−O peak at a reduced distance of 1.55 Å from the CoO_6 octahedral framework of pyrochlore due to the substitution of Co cations for the B-site (Figure 7f).[78] With the increase of applied potential, this peak remained constant possibly due to the rigid CoO_6 octahedral frameworks, whereas a new peak of the Co−O bond from CoOOH appeared at a reduced distance of 1.44 Å.[78] Moreover, the metallic Co−Co bond from Co nanoparticles was transformed into that of the edge-sharing Co^{3+} in CoOOH during the OER process. Both observations clearly indicate the conversion of metallic Co to CoOOH during the OER process.[78] Based on these *in situ* XAS characterizations, the superior OER activity of YRCO-560 was attributed to the synergetic contributions of (1) the facilitated oxidation of metallic Co to CoOOH on the pyrochlore oxide surface, which is often considered as the rate-determining step of the OER, and (2) the facile oxidation characteristic of both A-site Y and B-site Ru cations in pyrochlore oxide that can promote the efficient charge transfer from the oxidation of transition metal toward the inner layers of the support during the OER (Figure 7g).[78] The introduced pyrochlore-support-based hybrid catalyst is underexplored, and it may allow for designing high-performance electrocatalysts for other reactions including ORR and hydrogen evolution reaction (HER) through favorable interactions between metal nanoparticles and pyrochlore oxide supports.

The introduced pyrochlore-support-based hybrid catalyst is underexplored, and it may allow for designing high-performance electrocatalysts for other reactions including ORR and hydrogen evolution reaction (HER) through favorable interactions between metal nanoparticles and pyrochlore oxide supports.

OUTLOOK

Various combinations of A-site and B-site compositions of pyrochlore oxides, including cation doping, offer a myriad of opportunities to engineer the OER mechanisms and performance through fine-tuning the electronic structure and the surface adsorption energies of oxygen intermediates. Given the numerous combinations of pyrochlore oxide candidates, a computer-simulation-based screening process is extremely helpful in identifying the ideal structure of materials that can have superior catalytic activity and stability. A recent study first showed that the computational approach could be used to identify suitable pyrochlore oxides as OER catalysts based on the calculations of the phase, Pourbaix, and band energy diagrams and projected density of states.[31] Such a computational approach is highly needed to establish the structure−mechanism−performance relationship of pyrochlore oxides for specific electrochemical reactions.

Although significant advances have been achieved in designing high-performance pyrochlore oxide catalysts for OER under both acidic and alkaline conditions, a fundamental understanding of the OER mechanisms associated with the structure of pyrochlore is still largely lacking in comparison to other metal oxide catalysts. In particular, understanding the LOM mechanism involving the oxidation of the lattice oxygen of pyrochlore oxides remains a critical task. A recent study first revealed that the contribution of the LOM mechanism to the highly crystalline pyrochlore is negligible.[31] If the conventional AEM mechanism dominates highly crystalline metal oxides, facet engineering is crucial to improve the OER activity through the controlled surface atomic structure.[66] A recent study reported the correlation between low-index facets of micrometer-sized polyhedral pyrochlore ($Bi_2Ru_2O_7$) and their ORR and OER activities,[3] suggesting a new design strategy of pyrochlore oxides through facet engineering. On the other hand, in the case of doped pyrochlores containing large amounts of oxygen vacancies, the role of the LOM mechanism may be significant. A recent study has hypothesized that the increased oxygen lability and surface density of OV in metal-doped pyrochlores favors the LOM mechanism.[34] Thus, in-depth experimental and computational investigations should focus on revealing the active sites, including involvement of lattice oxygens, and the OER mechanisms, providing more guidelines for the discovery of pyrochlore oxides that can overcome the scaling limitations of the traditional OER mechanism. In addition, more *in situ* and *operando* analyses are needed to probe the surface structural changes of pyrochlore oxides and the corresponding reaction mechanism under OER conditions.

The role of pyrochlore oxides can be further increased when used as a conductive support material for other metal catalysts, because it can not only directly participate in the OER reaction but also efficiently transfer charges for facile oxidation of anchored metal catalysts. Recently, we have demonstrated that metallic Co nanoparticles anchored yttrium ruthenate pyrochlore oxide prepared by the *in situ* exsolution process can exhibit excellent OER activity. The superior OER activity of this hybrid catalyst is due to the facile oxidation of metallic Co to CoOOH by efficient charge transfer from the transition metal to the inner layers of the pyrochlore oxide support. Based on the same strategy, various transition metals or their alloy nanoparticles can be further synthesized on the pyrochlore oxide support by carefully controlling the reduction temperature. Such a significant advantage allows for the design of new pyrochlore-based hybrid catalysts capable of catalyzing specific electrochemical reactions, including ORR and HER. The synthesis of Ni and NiRu alloy nanoparticles on pyrochlore oxides is under investigation to design highly active catalysts for OER and HER.

https://dx.doi.org/10.1021/acscentsci.0c00479
ACS Cent. Sci. 2020, 6, 880−891

AUTHOR INFORMATION

Corresponding Authors

Myeongjin Kim − *Department of Hydrogen & Renewable Energy, Kyungpook National University, Daegu 41566, Republic of Korea*; Email: myeongjinkim@knu.ac.kr

Seung Woo Lee − *G. W. Woodruff School of Mechanical Engineering, Georgia Institute of Technology, Atlanta, Georgia 30332, United States*; orcid.org/0000-0002-2695-7105; Email: seung.lee@me.gatech.edu

Authors

Jinho Park − *G. W. Woodruff School of Mechanical Engineering, Georgia Institute of Technology, Atlanta, Georgia 30332, United States*

Minsoo Kang − *School of Materials Science and Engineering, Georgia Institute of Technology, Atlanta, Georgia 30332, United States*

Jin Young Kim − *Fuel Cell Research Center, Korea Institute of Science and Technology (KIST), Seoul 02792, Republic of Korea*; orcid.org/0000-0003-4822-3804

Complete contact information is available at: https://pubs.acs.org/10.1021/acscentsci.0c00479

Notes

The authors declare no competing financial interest.

ACKNOWLEDGMENTS

This work was supported by the Korea Institute of Energy Technology Evaluation and Planning (KETEP) grant funded by the Korea government (MOTIE) (No. 20188550000440).

REFERENCES

(1) Lewis, N. S.; Nocera, D. G. Powering the planet: Chemical challenges in solar energy utilization. *Proc. Natl. Acad. Sci. U. S. A.* **2006**, *103*, 15729−15735.

(2) Suntivich, J.; May, K. J.; Gasteiger, H. A.; Goodenough, J. B.; Shao-Horn, Y. A perovskite oxide optimized for oxygen evolution catalysis from molecular orbital principles. *Science* **2011**, *334*, 1383−1385.

(3) Fabbri, E.; Schmidt, T. J. Oxygen Evolution Reaction—The Enigma in Water Electrolysis. *ACS Catal.* **2018**, *8*, 9765−9774.

(4) Park, S.; Shao, Y.; Liu, J.; Wang, Y. Oxygen electrocatalysts for water electrolyzers and reversible fuel cells: status and perspective. *Energy Environ. Sci.* **2012**, *5*, 9331−9344.

(5) Grimaud, A.; Diaz-Morales, O.; Han, B.; Hong, W. T.; Lee, Y.-L.; Giordano, L.; Stoerzinger, K. A.; Koper, M. T.; Shao-Horn, Y. Activating lattice oxygen redox reactions in metal oxides to catalyse oxygen evolution. *Nat. Chem.* **2017**, *9*, 457−465.

(6) Grimaud, A.; May, K. J.; Carlton, C. E.; Lee, Y.-L.; Risch, M.; Hong, W. T.; Zhou, J.; Shao-Horn, Y. Double perovskites as a family of highly active catalysts for oxygen evolution in alkaline solution. *Nat. Commun.* **2013**, *4*, 2439.

(7) Huynh, M.; Bediako, D. K.; Nocera, D. G. A functionally stable manganese oxide oxygen evolution catalyst in acid. *J. Am. Chem. Soc.* **2014**, *136*, 6002−6010.

(8) Lee, Y.; Suntivich, J.; May, K. J.; Perry, E. E.; Shao-Horn, Y. Synthesis and activities of rutile IrO_2 and RuO_2 nanoparticles for oxygen evolution in acid and alkaline solutions. *J. Phys. Chem. Lett.* **2012**, *3*, 399−404.

(9) Rossmeisl, J.; Qu, Z.-W.; Zhu, H.; Kroes, G.-J.; Nørskov, J. K. Electrolysis of water on oxide surfaces. *J. Electroanal. Chem.* **2007**, *607*, 83−89.

(10) Xiang, C.; Papadantonakis, K. M.; Lewis, N. S. Principles and implementations of electrolysis systems for water splitting. *Mater. Horiz.* **2016**, *3*, 169−173.

(11) Cheng, X.; Fabbri, E.; Nachtegaal, M.; Castelli, I. E.; Kazzi, M. E.; Haumont, R.; Marzari, N.; Schmidt, T. J. Oxygen evolution reaction on $La_{1-x}Sr_xCoO_3$ perovskites: a combined experimental and theoretical study of their structural, electronic, and electrochemical properties. *Chem. Mater.* **2015**, *27*, 7662−7672.

(12) Cheng, X.; Fabbri, E.; Yamashita, Y.; Castelli, I. E.; Kim, B.; Uchida, M.; Haumont, R.; Puente-Orench, I.; Schmidt, T. J. Oxygen evolution reaction on perovskites: A multieffect descriptor study combining experimental and theoretical methods. *ACS Catal.* **2018**, *8*, 9567−9578.

(13) Man, I. C.; Su, H. Y.; Calle-Vallejo, F.; Hansen, H. A.; Martinez, J. I.; Inoglu, N. G.; Kitchin, J.; Jaramillo, T. F.; Nørskov, J. K.; Rossmeisl, J. Universality in oxygen evolution electrocatalysis on oxide surfaces. *ChemCatChem* **2011**, *3*, 1159−1165.

(14) Seitz, L. C.; Dickens, C. F.; Nishio, K.; Hikita, Y.; Montoya, J.; Doyle, A.; Kirk, C.; Vojvodic, A.; Hwang, H. Y.; Norskov, J. K.; Jaramillo, T. F. A highly active and stable $IrO_x/SrIrO_3$ catalyst for the oxygen evolution reaction. *Science* **2016**, *353*, 1011−1014.

(15) Lebedev, D.; Povia, M.; Waltar, K.; Abdala, P. M.; Castelli, I. E.; Fabbri, E.; Blanco, M. V.; Fedorov, A.; Copéret, C.; Marzari, N.; Schmidt, T. J. Highly Active and Stable Iridium Pyrochlores for Oxygen Evolution Reaction. *Chem. Mater.* **2017**, *29*, 5182−5191.

(16) Danilovic, N.; Subbaraman, R.; Chang, K.-C.; Chang, S. H.; Kang, Y. J.; Snyder, J.; Paulikas, A. P.; Strmcnik, D.; Kim, Y.-T.; Myers, D.; Stamenkovic, V. R.; Markovic, N. M. Activity−Stability Trends for the Oxygen Evolution Reaction on Monometallic Oxides in Acidic Environments. *J. Phys. Chem. Lett.* **2014**, *5*, 2474−2478.

(17) Yang, L.; Yu, G.; Ai, X.; Yan, W.; Duan, H.; Chen, W.; Li, X.; Wang, T.; Zhang, C.; Huang, X.; Chen, J.-S.; Zou, X. Efficient oxygen evolution electrocatalysis in acid by a perovskite with face-sharing IrO_6 octahedral dimers. *Nat. Commun.* **2018**, *9*, 5236.

(18) Chen, Y.; Li, H.; Wang, J.; Du, Y.; Xi, S.; Sun, Y.; Sherburne, M.; Ager, J. W.; Fisher, A. C.; Xu, Z. J. Exceptionally active iridium evolved from a pseudo-cubic perovskite for oxygen evolution in acid. *Nat. Commun.* **2019**, *10*, 572.

(19) Liang, X.; Shi, L.; Liu, Y.; Chen, H.; Si, R.; Yan, W.; Zhang, Q.; Li, G.-D.; Yang, L.; Zou, X. Activating Inert, Nonprecious Perovskites with Iridium Dopants for Efficient Oxygen Evolution Reaction under Acidic Conditions. *Angew. Chem., Int. Ed.* **2019**, *58*, 7631−7635.

(20) Retuerto, M.; Pascual, L.; Calle-Vallejo, F.; Ferrer, P.; Gianolio, D.; Pereira, A. G.; García, Á.; Torrero, J.; Fernández-Díaz, M. T.; Bencok, P.; Peña, M. A.; Fierro, J. L. G.; Rojas, S. Na-doped ruthenium perovskite electrocatalysts with improved oxygen evolution activity and durability in acidic media. *Nat. Commun.* **2019**, *10*, 2041.

(21) Zhang, R.; Pearce, P. E.; Pimenta, V.; Cabana, J.; Li, H.; Corte, D. A. D.; Abakumov, A. M.; Rousse, G.; Giaume, D.; Deschamps, M.; Grimaud, A. First Example of Protonation of Ruddlesden−Popper Sr_2IrO_4: A Route to Enhanced Water Oxidation Catalysts. *Chem. Mater.* **2020**, *32*, 3499−3509.

(22) Sardar, K.; Petrucco, E.; Hiley, C. I.; Sharman, J. D. B.; Wells, P. P.; Russell, A. E.; Kashtiban, R. J.; Sloan, J.; Walton, R. I. Water-Splitting Electrocatalysis in Acid Conditions Using Ruthenate-Iridate Pyrochlores. *Angew. Chem.* **2014**, *126*, 11140−11144.

(23) Feng, Q.; Wang, Q.; Zhang, Z.; Xiong, Y.; Li, H.; Yao, Y.; Yuan, X.-Z.; Williams, M. C.; Gu, M.; Chen, H.; Li, H.; Wang, H. Highly active and stable ruthenate pyrochlore for enhanced oxygen evolution reaction in acidic medium electrolysis. *Appl. Catal., B* **2019**, *244*, 494−501.

(24) Pi, Y.; Zhang, N.; Guo, S.; Guo, J.; Huang, X. Ultrathin laminar Ir superstructure as highly efficient oxygen evolution electrocatalyst in broad pH range. *Nano Lett.* **2016**, *16*, 4424−4430.

(25) Zhu, J.; Chen, Z.; Xie, M.; Lyu, Z.; Chi, M.; Mavrikakis, M.; Jin, W.; Xia, Y. Iridium-Based Cubic Nanocages with 1.1-nm-Thick Walls: A Highly Efficient and Durable Electrocatalyst for Water Oxidation in an Acidic Medium. *Angew. Chem., Int. Ed.* **2019**, *58*, 7244−7248.

(26) Antolini, E. Iridium as catalyst and cocatalyst for oxygen evolution/reduction in acidic polymer electrolyte membrane electrolyzers and fuel cells. *ACS Catal.* **2014**, *4*, 1426−1440.

(27) Sardar, K.; Ball, S. C.; Sharman, J. D.; Thompsett, D.; Fisher, J. M.; Smith, R. A.; Biswas, P. K.; Lees, M. R.; Kashtiban, R. J.; Sloan, J.; Walton, R. I. Bismuth iridium oxide oxygen evolution catalyst from hydrothermal synthesis. *Chem. Mater.* **2012**, *24*, 4192−4200.
(28) Kim, J.; Shih, P.-C.; Tsao, K.-C.; Pan, Y.-T.; Yin, X.; Sun, C.-J.; Yang, H. High-performance pyrochlore-type yttrium ruthenate electrocatalyst for oxygen evolution reaction in acidic media. *J. Am. Chem. Soc.* **2017**, *139*, 12076−12083.
(29) Shih, P.-C.; Kim, J.; Sun, C.-J.; Yang, H. Single-phase pyrochlore $Y_2Ir_2O_7$ electrocatalyst on the activity of oxygen evolution reaction. *ACS Appl. Energy Mater.* **2018**, *1*, 3992−3998.
(30) Kim, J.; Shih, P.-C.; Qin, Y.; Al-Bardan, Z.; Sun, C.-J; Yang, H. A Porous Pyrochlore Y_2 $[Ru_{1.6}Y_{0.4}]$ $O_{7-\delta}$ Electrocatalyst for Enhanced Performance towards the Oxygen Evolution Reaction in Acidic Media. *Angew. Chem.* **2018**, *130*, 14073−14077.
(31) Abbott, D. F.; Pittkowski, R. K.; Macounova, K.; Nebel, R.; Marelli, E.; Fabbri, E.; Castelli, I. E.; Krtil, P.; Schmidt, T. J. Design and Synthesis of Ir/Ru Pyrochlore Catalysts for the Oxygen Evolution Reaction Based on Their Bulk Thermodynamic Properties. *ACS Appl. Mater. Interfaces* **2019**, *11*, 37748−37760.
(32) Feng, Q.; Zou, J.; Wang, Y.; Zhao, Z.; Williams, M. C.; Li, H.; Wang, H. Influence of Surface Oxygen Vacancies and Ruthenium Valence State on the Catalysis of Pyrochlore Oxides. *ACS Appl. Mater. Interfaces* **2020**, *12*, 4520−4530.
(33) Shang, C.; Cao, C.; Yu, D.; Yan, Y.; Lin, Y.; Li, H.; Zheng, T.; Yan, X.; Yu, W.; Zhou, S.; Zeng, J. Electron correlations engineer catalytic activity of pyrochlore iridates for acidic water oxidation. *Adv. Mater.* **2018**, *31*, 1805104.
(34) Kuznetsov, D. A.; Naeem, M. A.; Kumar, P. V.; Abdala, P. M.; Fedorov, A.; Müller, C. R. Tailoring Lattice Oxygen Binding in Ruthenium Pyrochlores to Enhance Oxygen Evolution Activity. *J. Am. Chem. Soc.* **2020**, *142*, 7883−7888.
(35) Park, J.; Risch, M.; Nam, G.; Park, M.; Shin, T. J.; Park, S.; Kim, M. G.; Shao-Horn, Y.; Cho, J. Single crystalline pyrochlore nanoparticles with metallic conduction as efficient bi-functional oxygen electrocatalysts for Zn−air batteries. *Energy Environ. Sci.* **2017**, *10*, 129−136.
(36) Park, J.; Park, M.; Nam, G.; Kim, M. G.; Cho, J. Unveiling the Catalytic Origin of Nanocrystalline Yttrium Ruthenate Pyrochlore as a Bifunctional Electrocatalyst for Zn−Air Batteries. *Nano Lett.* **2017**, *17*, 3974−3981.
(37) Park, J.; Shirai, M.; Jung, G. Y.; Park, S. O.; Park, M.; Ryu, J.; Kwak, S. K.; Cho, J. Correlation of Low-Index Facets to Active Sites in Micrometer-Sized Polyhedral Pyrochlore Electrocatalyst. *ACS Catal.* **2018**, *8*, 9647−9655.
(38) Parrondo, J.; George, M.; Capuano, C.; Ayers, K. E.; Ramani, V. Pyrochlore electrocatalysts for efficient alkaline water electrolysis. *J. Mater. Chem. A* **2015**, *3*, 10819−10828.
(39) Sidi Ahmed, O. A.; Bourja, L.; Chagraoui, A.; Tairi, A.; Moussaoui, A.; Oulahyane, H. A.; Manoun, B.; Villain, S. Characterization and densification of defect pyrochlore oxide powders $ABi_2Ta_5O_{16}$ (A= Na, Tl). *Heliyon* **2019**, *5*, e01628.
(40) Subramanian, M.; Aravamudan, G.; Rao, G. S. Oxide pyrochlores—A Review. *Prog. Solid State Chem.* **1983**, *15*, 55−143.
(41) Jitta, R. R.; Gundeboina, R.; Veldurthi, N. K.; Guje, R.; Muga, V. Defect pyrochlore oxides: as photocatalyst materials for environmental and energy applications-a review. *J. Chem. Technol. Biotechnol.* **2015**, *90*, 1937−1948.
(42) Bouchard, R.; Gillson, J. A new family of bismuth—precious metal pyrochlores. *Mater. Res. Bull.* **1971**, *6*, 669−679.
(43) Longo, J.; Raccah, P. M.; Goodenough, J. B. $Pb_2M_2O_{7-x}$(M= Ru, Ir, Re)—Preparation and properties of oxygen deficient pyrochlores. *Mater. Res. Bull.* **1969**, *4*, 191−202.
(44) Cox, P. A.; Egdell, R. G.; Goodenough, J. B.; Hamnett, A.; Naish, C. The metal-to-semiconductor transition in ternary ruthenium (IV) oxides: a study by electron spectroscopy. *J. Phys. C: Solid State Phys.* **1983**, *16*, 6221−6239.
(45) Akazawa, T.; Inaguma, Y.; Katsumata, T.; Hiraki, K.; Takahashi, T. Flux Growth and Physical Properties of Pyrochlore $Pb_2Ru_2O_{6.5}$ Single Crystals. *J. Cryst. Growth* **2004**, *271*, 445−449.
(46) Lee, K.-S.; Seo, D.-K.; Whangbo, M.-H. Structural and Electronic Factors Governing the Metallic and Nonmetallic Properties of the Pyrochlores $A_2Ru_2O_{7-y}$. *J. Solid State Chem.* **1997**, *131*, 405−408.
(47) Goodenough, J. B.; Manoharan, R.; Paranthaman, M. Surface protonation and electrochemical activity of oxides in aqueous solution. *J. Am. Chem. Soc.* **1990**, *112*, 2076−2082.
(48) Gökağaş, G.; Kennedy, B. J. Potential-dependent surface segregation in lead+ ruthenium pyrochlore $Pb_2Ru_2O_{7-y}$. *J. Electroanal. Chem.* **1993**, *353*, 71−80.
(49) Gökağaç, G.; Kennedy, B. J. Oxidative stability of bismuth-ruthenium pyrochlore $Bi_2Ru_2O_{7-y}$. *J. Electroanal. Chem.* **1994**, *368*, 235−239.
(50) ten Kortenaar, M.V.; Vente, J.F.; Ijdo, D.J.W.; Müller, S.; Kötz, R. Oxygen evolution and reduction on iridium oxide compounds. *J. Power Sources* **1995**, *56*, 51−60.
(51) Oh, S. H.; Adams, B. D.; Lee, B.; Nazar, L. F. Direct, Soft Chemical Route to Mesoporous Metallic Lead Ruthenium Pyrochlore and Investigation of its Electrochemical Properties. *Chem. Mater.* **2015**, *27*, 2322−2331.
(52) Kim, M.; Ju, H.; Kim, J. Dihydrogen phosphate ion functionalized nanocrystalline thallium ruthenium oxide pyrochlore as a bifunctional electrocatalyst for aqueous Na-air batteries. *Appl. Catal., B* **2019**, *245*, 29−39.
(53) Hammer, B.; Nørskov, J. K. Theoretical surface science and catalysis—calculations and concepts. *Adv. Catal.* **2000**, *45*, 71−129.
(54) Grimaud, A.; Hong, W. T.; Shao-Horn, Y.; Tarascon, J.-M. Anionic redox processes for electrochemical devices. *Nat. Mater.* **2016**, *15*, 121−126.
(55) Grimaud, A.; Demortière, A.; Saubanère, M.; Dachraoui, W.; Duchamp, M.; Doublet, M.-L.; Tarascon, J.-M. Activation of surface oxygen sites on an iridium-based model catalyst for the oxygen evolution reaction. *Nat. Energy* **2017**, *2*, 16189.
(56) Berti, G.; Sanna, S.; Castellano, C.; Duijn, J. V.; Ruiz-Bustos, R.; Bordonali, L.; Bussetti, G.; Calloni, A.; Demartin, F.; Duò, L.; Brambilla, A. Observation of Mixed Valence Ru Components in Zn Doped $Y_2Ru_2O_7$ Pyrochlores. *J. Phys. Chem. C* **2016**, *120*, 11763−11768.
(57) Yoshii, S.; Murata, K.; Sato, M. Metal−insulator transition of $R_{2-x}Ca_xRu_2O_7$ (R= Y, Sm). *J. Phys. Chem. Solids* **2001**, *62*, 129−134.
(58) Pirzada, M.; Grimes, R. W.; Maguire, J. F. Incorporation of divalent ions in $A_2B_2O_7$ pyrochlores. *Solid State Ionics* **2003**, *161*, 81−91.
(59) Feng, Q.; Zhao, Z.; Yuan, X.-Z.; Li, H.; Wang, H. Oxygen vacancy engineering of yttrium ruthenate pyrochlores as an efficient oxygen catalyst for both proton exchange membrane water electrolyzers and rechargeable zinc-air batteries. *Appl. Catal., B* **2020**, *260*, 118176.
(60) Feng, Q.; Zhang, Z.; Huang, H.; Yao, K.; Fan, J.; Zeng, L.; Williams, M. C.; Li, H.; Wang, H. An effective strategy to tune the oxygen vacancy of pyrochlore oxides for electrochemical energy storage and conversion systems. *Chem. Eng. J.* **2020**, *395*, 124428.
(61) Hong, W. T.; Stoerzinger, K. A.; Lee, Y.-L.; Giordano, L.; Grimaud, A.; Johnson, A. M.; Hwang, J.; Crumlin, E. J.; Yang, W.; Shao-Horn, Y. Charge-transfer-energy-dependent oxygen evolution reaction mechanisms for perovskite oxides. *Energy Environ. Sci.* **2017**, *10*, 2190−2200.
(62) Lee, Y.-L.; Kleis, J.; Rossmeisl, J.; Shao-Horn, Y.; Morgan, D. Prediction of solid oxide fuel cell cathode activity with first-principles descriptors. *Energy Environ. Sci.* **2011**, *4*, 3966−3970.
(63) Binninger, T.; Mohamed, R.; Waltar, K.; Fabbri, E.; Levecque, P.; Kötz, R.; Schmidt, T. J. Thermodynamic explanation of the universal correlation between oxygen evolution activity and corrosion of oxide catalysts. *Sci. Rep.* **2015**, *5*, 12167.
(64) Mefford, J. T.; Rong, X.; Abakumov, A. M.; Hardin, W. G.; Dai, S.; Kolpak, A. M.; Johnston, K. P.; Stevenson, K. J. Water electrolysis on $La_{1-x}Sr_xCoO_{3-\delta}$ perovskite electrocatalysts. *Nat. Commun.* **2016**, *7*, 11053.

https://dx.doi.org/10.1021/acscentsci.0c00479
ACS Cent. Sci. 2020, 6, 880−891

(65) Yoo, J. S.; Rong, X.; Liu, Y.; Kolpak, A. M. Role of Lattice Oxygen Participation in Understanding Trends in the Oxygen Evolution Reaction on Perovskites. *ACS Catal.* **2018**, *8*, 4628−4636.
(66) Stoerzinger, K. A.; Diaz-Morales, O.; Kolb, M.; Rao, R. R.; Frydendal, R.; Qiao, L.; Wang, X. R.; Halck, N. B.; Rossmeisl, J.; Hansen, H. A. Orientation-Dependent Oxygen Evolution on RuO_2 without Lattice Exchange. *ACS Energy Lett.* **2017**, *2*, 876−881.
(67) Rong, X.; Parolin, J.; Kolpak, A. M. A Fundamental Relationship between Reaction Mechanism and Stability in Metal Oxide Catalysts for Oxygen Evolution. *ACS Catal.* **2016**, *6*, 1153−1158.
(68) Fabbri, E.; Nachtegaal, M.; Binninger, T.; Cheng, X.; Kim, B.-J.; Durst, J.; Bozza, F.; Graule, T.; Schäublin, R.; Wiles, L.; Pertoso, M.; Danilovic, N.; Ayers, K. E.; Schmidt, T. J. Dynamic surface self-reconstruction is the key of highly active perovskite nano-electrocatalysts for water splitting. *Nat. Mater.* **2017**, *16*, 925−931.
(69) Oh, H.-S.; Nong, H. N.; Strasser, P. Preparation of Mesoporous Sb-, F-, and In-Doped SnO_2 Bulk Powder with High Surface Area for Use as Catalyst Supports in Electrolytic Cells. *Adv. Funct. Mater.* **2015**, *25*, 1074−1081.
(70) Sui, S.; Wang, X.; Zhou, X.; Su, Y.; Riffat, S.; Liu, C.-J. A comprehensive review of Pt electrocatalysts for the oxygen reduction reaction: Nanostructure, activity, mechanism and carbon support in PEM fuel cells. *J. Mater. Chem. A* **2017**, *5*, 1808−1825.
(71) Castanheira, L.; Silva, W. O.; Lima, F. H. B.; Crisci, A.; Dubau, L.; Maillard, F. Carbon Corrosion in Proton-Exchange Membrane Fuel Cells: Effect of the Carbon Structure, the Degradation Protocol, and the Gas Atmosphere. *ACS Catal.* **2015**, *5*, 2184−2194.
(72) Nong, H. N.; Oh, H.-S.; Reier, T.; Willinger, E.; Willinger, M.-G.; Petkov, V.; Teschner, D.; Strasser, P. Oxide-Supported $IrNiO_x$ Core−Shell Particles as Efficient, Cost-Effective, and Stable Catalysts for Electrochemical Water Splitting. *Angew. Chem., Int. Ed.* **2015**, *54*, 2975−2979.
(73) Kim, J.; Chen, X.; Pan, Y. T.; Shih, P. C.; Yang, H. W-Doped $CaMnO_{2.5}$ and $CaMnO_3$ Electrocatalysts for Enhanced Performance in Oxygen Evolution and Reduction Reactions. *J. Electrochem. Soc.* **2017**, *164*, F1074−F1080.
(74) Zhu, W. K.; Wang, M.; Seradjeh, B.; Yang, F.; Zhang, S. X. Enhanced weak ferromagnetism and conductivity in hole-doped pyrochlore iridate $Y_2Ir_2O_7$. *Phys. Rev. B: Condens. Matter Mater. Phys.* **2014**, *90*, 054419.
(75) Oh, S. H.; Black, R.; Pomerantseva, E. A.; Lee, J.-H.; Nazar, L. F. Synthesis of a metallic mesoporous pyrochlore as a catalyst for lithium−O_2 batteries. *Nat. Chem.* **2012**, *4*, 1004−1010.
(76) Lee, K. T.; Lee, B. W.; Camaratta, M. A.; Wachsman, E. D. Enhanced oxygen reduction reaction with nano-scale pyrochlore bismuth ruthenate via cost-effective wet-chemical synthesis. *RSC Adv.* **2013**, *3*, 19866−19871.
(77) Shih, P.-C.; Zhang, C.; Raheja, H.; Sun, C.-J.; Yang, H. Polymer Entrapment Flash Pyrolysis for the Preparation of Nanoscale Iridium-Free Oxygen Evolution Electrocatalysts. *ChemNanoMat* **2020**, *6*, 930−936.
(78) Kim, M.; Lee, B.; Ju, H.; Lee, S. W.; Kim, J. Reducing the Barrier Energy of Self-Reconstruction for Anchored Cobalt Nanoparticles as Highly Active Oxygen Evolution Electrocatalyst. *Adv. Mater.* **2019**, *31*, 1901977.

https://dx.doi.org/10.1021/acscentsci.0c00479
ACS Cent. Sci. 2020, 6, 880−891